Polymorphism

DOI: 10.1002/anie.200804563

Reversible Phase Transitions in a Buckybowl Monolayer**

*Leo Merz, Manfred Parschau, Laura Zoppi, Kim K. Baldridge, Jay S. Siegel, and Karl-Heinz Ernst**

Many chemical compounds exist in more than one crystalline form; however, the reasons for the appearance of different polymorphs during crystallization are still largely unknown. Polymorphism in general, and the inability to control it[1] in particular, have tremendous technological and commercial consequences in fields such as pharmaceutical[2] and materials science.[3] The first observation of a transformation between two different polymorphs of an organic compound dates back to 1832, when Liebig and Wöhler reported the conversion of silky needles of benzamide into rhombic crystals.[4] However, the mechanisms involved in such molecular solid-state phase transitions remain poorly understood. The origin of polymorphism has been attributed to kinetically controlled nucleation and growth, and many thermodynamically unstable polymorphs, such as diamond and cocoa butter in chocolate, are used daily in their metastable form.[5] On the other hand, materials may appear in several thermodynamically stable crystal modifications that can be interconverted reversibly with changing temperature.[6] These so-called enantiotropic phase transitions are equally poorly understood, and there is much debate about the mechanisms involved.[7] They are commonly described by global thermodynamics and kinetics, but rarely at the microscopic level.[8] In particular, the lattice dynamics before and during the transition can not be investigated satisfactorily by experimental approaches such as X-ray crystallography and solid-state NMR spectroscopy. These methods deliver exact averaged structures, but very little information about the motion of individual atoms and molecules.[9]

It is easier to monitor and understand phase transitions in two dimensions on surfaces, as they can be followed at the molecular level with a scanning tunneling microscope. In the 25-year period since its invention, scanning tunneling microscopy (STM) has been helpful in the discovery of a wealth of phenomena in diverse atomic and molecular systems.[10] Herein we report temperature-controlled, reversible phase transitions in a two-dimensional (2D) molecular crystal of the bowl-shaped geodesic fullerene fragment molecule corannulene on a copper surface under ultrahigh-vacuum conditions. Upon cooling, the room-temperature phase undergoes contraction into a denser crystal phase, followed by rearrangement into yet another phase at lower temperatures. Heating restores the higher-temperature phases successively (Figure 1). Lattice instabilities in the form of periodic displacements of lattice row segments are observed directly in the supercooled state before the onset of the first transition. The stability against lattice contraction at room temperature is explained by breathing-mode vibrations of the bowl molecule. The depopulation of these vibrational states upon cooling enables attractive intermolecular forces to become more effective, which causes the phase transition.

Copper(111) provides an ideal surface for thin films of aromatic molecules because of the perfect match between the

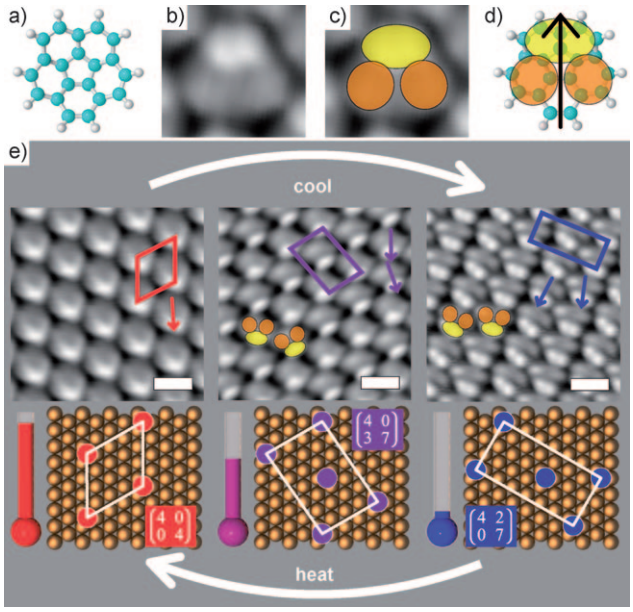

Figure 1. Reversible phase transitions in two dimensions. a) Ball-and-stick model of corannulene. b–d) The correlation of the STM contrast at low temperatures with the molecular structure reveals a tilted adsorption geometry. The two top-most hexagonal rings (yellow) are imaged as bright protrusions, and the two middle rings (orange) appear with medium brightness. e) Top: STM images of the three observed phases (averaged from 186, 64, and 17 different positions, respectively, from left to right). The unit cells and the molecular azimuthal orientations are indicated. Scale bars: 1 nm. Bottom: The unit cells on the copper grid are shown with their matrix notation. Upon cooling, a (4 0, 0 4) lattice rearranges to give first a (4 0, 3 7) phase and then a (4 2, 0 7) phase. The original phase forms again upon heating.

[*] Dr. L. Merz, Dr. M. Parschau, Dr. K.-H. Ernst
Nanoscale Materials Science, Swiss Federal Laboratories for Materials Testing and Research (Empa)
Überlandstrasse 129, 8600 Dübendorf (Switzerland)
Fax: (+41) 44-823-4034
E-mail: karl-heinz.ernst@empa.ch
Homepage: http://www.empa.ch/mss
L. Zoppi, Prof. Dr. K. K. Baldridge, Prof. Dr. J. S. Siegel, Dr. K.-H. Ernst
Organisch-chemisches Institut, Universität Zürich (Switzerland)

[**] Financial support by the Schweizerischer Nationalfonds for the project FUNDASA is gratefully acknowledged. We thank Prof. Jack Dunitz for fruitful discussions.

Supporting information for this article is available on the WWW under http://dx.doi.org/10.1002/anie.200804563.

size of hexagonal C_6 rings and the substrate lattice.[11] The molecule corannulene ($C_{20}H_{10}$) is a curved, C_{5v}-symmetric aromatic molecule (Figure 1a) with a pentagonal ring centered among hexagonal rings and thus represents a segment of C_{60} buckminsterfullerene.[12] At room temperature, a regular (4 0, 0 4) array is observed for the complete corannulene monolayer (Figure 1e).[13] Upon cooling, the 2D crystal undergoes two different phase transitions. A denser (4 0, 3 7) lattice forms at 225 K, and a (4 2, 0 7) structure forms upon a further decrease in temperature. Each structure is stable in its respective temperature interval, as confirmed by the reversibility of the transitions: The medium-temperature phase forms again when the low-temperature phase is heated, and is then converted completely into the (4 0, 0 4) phase at room temperature. To our knowledge, this is the first observation of an enantiotropic phase transition in a 2D organic molecular crystal. Both transitions show a hysteresis in temperature. The (4 0, 3 7) structure exists at temperatures between 201 and 248 K. The highest temperature observed for the (4 2, 0 7) structure was 236 K upon cooling and 271 K during heating (see Figure S1 in the Supporting Information). This overlap of temperature ranges indicates that it should be possible to convert the (4 0, 0 4) phase directly into the (4 2, 0 7) phase and vice versa, as occasionally observed in this study. However, in these cases the transition could have passed too quickly through the (4 0, 3 7) phase to be resolved by STM. Nevertheless, coexistence of the two low-temperature phases—separated by a phase boundary containing highly mobile molecules—was observed regularly upon careful cooling (see Figure S2 in the Supporting Information).

Single molecules in all three phases appear asymmetrical by STM. This apparent asymmetry indicates a substantial tilt of the molecular bowl with respect to the surface plane. This geometry was confirmed by dispersion-corrected density functional theory (DFT-D) calculations, which showed that one of the five C_6 rings is oriented parallel to the surface above a threefold hollow site (see Figure S3 in the Supporting Information). Such an orientation has also been reported for C_{60} in its (4 0, 0 4) lattice on Cu(111).[14] With increasing intramolecular resolution at lower temperatures, a simple assignment of the upper and middle part of the molecules becomes possible (Figure 1b–d). In contrast to the (4 0, 0 4) structure, in which all molecules in a single domain have identical orientations (Figure 1e), the unit cells of the two low-temperature phases contain two molecules, each with different azimuthal orientations. The (4 0, 3 7) intermediate structure was identified by detailed statistical analysis of next-neighbor distances and lattice-vector directions in many STM images (see Figure S4 in the Supporting Information). The two molecules of the unit cell are located on different sites, namely, hexagonal-close-packed (hcp) and face-centered-cubic (fcc) threefold hollow sites.

The lattice density changes substantially during the (4 0, 0 4)/(4 0, 3 7) transition, but not for the (4 0, 3 7)/(4 2, 0 7) transition. The unit-cell area for the two lower-temperature phases is 1.94 nm^2 (28 Cu atoms) for two molecules and for the room-temperature phase 1.11 nm^2 (16 Cu surface atoms) for one molecule. Thus, upon cooling, with the same number of molecules on the surface, the lattice density is increased by 14.3%. Density changes in 3D solid-state phase transitions are usually of the order of a few percent.[15] One consequence of this lattice contraction is that other surface areas have a lower molecule density. Figure 2 shows an STM image taken at the boundary between such a low-density area and the

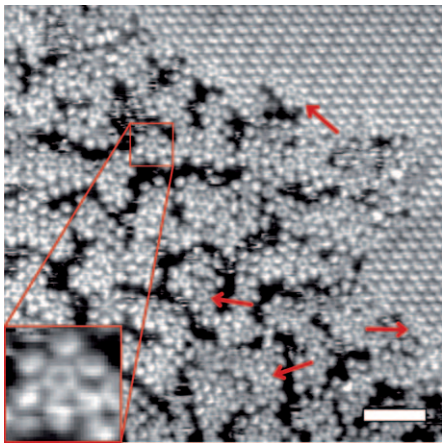

Figure 2. "Frozen 2D gas". The STM image shows the condensed (4 2, 0 7) lattice (top right) and a low-density disordered phase containing molecules that appear as perfect fivefold-symmetric doughnuts (red arrows), some of which are surrounded by six tilted molecules (inset). Scale bar: 5 nm. $T = 69$ K.

ordered crystal phase at 69 K. This coexistence is a result of a dynamic equilibrium between the crystal phase and a 2D gas. The new phase grows until the attachment–detachment equilibrium is reached. Molecules in the 2D gas phase are too mobile to be resolved with STM, but they freeze upon further cooling. When the sample is heated, the disordered area melts first at about 102 K. In strong contrast to the appearance of the molecules in the ordered crystal phases, many molecules in the disordered area appear as fivefold-symmetric doughnuts (Figure 2, red arrows, inset). This orientation agrees well with that found for corannulene on Cu(110) in the ordered lattice, in which the central pentagonal ring is essentially oriented parallel to the surface, and the bowl opening is pointing upwards.[16] These differences between the appearance of molecules in the lattice and the appearance of molecules in the disordered area strongly support our conclusion that the molecules in the ordered structures are substantially tilted (Figure 3a).

Two lattice directions and one intermolecular distance are identical in the (4 0, 0 4) and (4 0, 3 7) structures. The fact that two intermolecular distances became shorter in the transition to the (4 0, 3 7) structure is only compatible with compression along one direction of close-packed molecules (see Figure S4 in the Supporting Information).

When the (4 0, 0 4) phase becomes unstable upon slight supercooling below the equilibrium temperature, wiggling motions of molecules in every second row take place with a period of a few seconds (Figure 4a–d). That is, the STM images show double rows that form periodically in equivalent substrate lattice directions. The different contrast of the molecules in adjacent rows suggests that the motion involves a

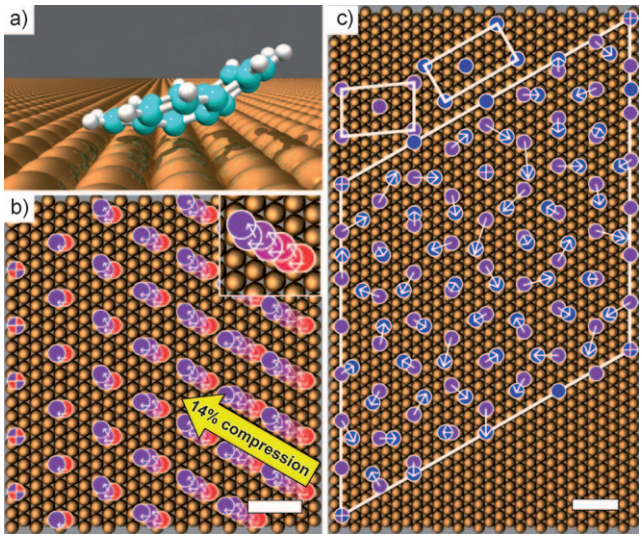

Figure 3. Mechanisms of the 2D phase transitions. a) Side view of a model of a single, tilted corannulene molecule adsorbed on Cu(111). b) Model of the transition from the (4 0, 0 4) structure (red) to the (4 0, 3 7) structure (purple). The nucleation site is the last row on the left-hand side, and the molecules move via the hcp and fcc sites (insert) along the $\langle\bar{1}10\rangle$ direction, whereby the 2D crystal becomes compressed by 14.3%. The distances migrated by the molecules differ and depend on the distance to the nucleation site. c) The (4 0, 3 7) lattice (purple) and the (4 2, 0 7) structure (blue) coincide in a (28 0, 0 28) supercell. Thearrows indicate a shortest-distance travel scenario. Scale bars: 1 nm.

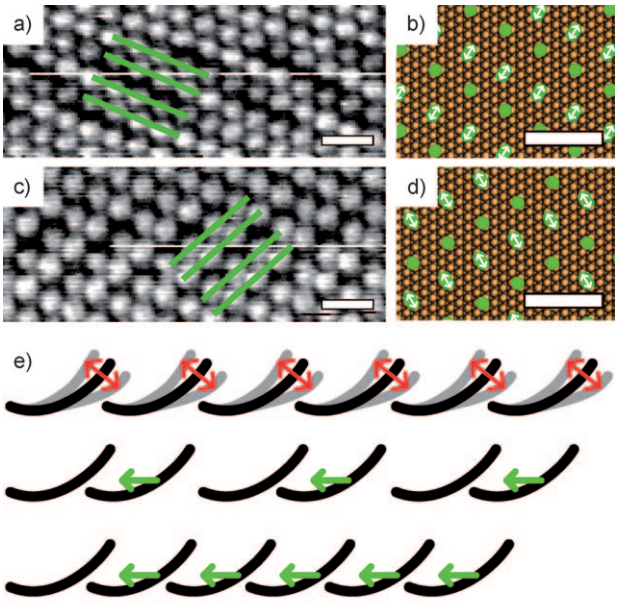

Figure 4. Lattice dynamics in the supercooled state. a–d) STM snapshots and schematic representations that show the wiggling motion of row segments in the supercooled (4 0, 0 4) phase at 221 K. In every second row, the molecules move closer to an adjacent row. As a result, the distances between the rows differ (green lines). The two STM images acquired in the same section of the lattice reveal the wiggling motion in equivalent directions. Scale bars: 2 nm. e) Sketches showing the increased spatial requirements of the molecular bowls vibrating at high temperature (top), the formation of pairs of rows in the supercooled state (middle), and the formation of the denser (4 0, 3 7) phase through the concerted migration of molecules over large distances (bottom).

site change from the favored fcc site to the next hcp site. These movements involve a zipperlike displacement of several adjacent molecules of a row. The wiggling motion can be rationalized as the simultaneous formation of many (4 0, 3 7) nuclei, but without starting the phase transition. Our proposed microscopic-scale mechanism for the phase transition takes these directly observed lattice dynamics in the supercooled (4 0, 0 4) phase into account: One single row acts as the nucleus (Figure 3b left, red/purple row). Starting with the wiggling step observed in the supercooled phase, molecules of the adjacent row move toward this row and cause the molecules to rotate azimuthally into the new alignment. The rest of the layer then follows step-by-step in the same direction, which results in mass transport along one $\langle\bar{1}10\rangle$ direction only. If the movement of the molecules during the phase transitions occurred in all three equal $\langle\bar{1}10\rangle$ directions simultaneously, one would expect to observe more and much smaller rotational domains after the transition. Rotational domains and their boundaries are observed (see Figure S5 in the Supporting Information); however, the usual domain sizes (a domain often covers a complete substrate terrace) support the hypothesis that all molecules of a single domain have moved along the same direction. We propose that the migration proceeds via the fcc and hcp threefold hollow sites (Figure 3b), as they have been identified by DFT-D calculations as the energetically most favored sites.

The second transition at lower temperature does not involve a change in density. The two lattices coincide in a (28 0, 0 28) superlattice (Figure 3c), and the molecules have to move only 3.6 Å on average. In the (4 0, 3 7) lattice, half of the molecules occupy a different—and therefore an energetically less favored—adsorption site. Our DFT-D results show that the fcc threefold hollow site is favored by 3.86 kJ mol^{-1} (0.04 eV) over the hcp site. Hence, the molecules switch to the more favored site and adopt a different azimuthal orientation to minimize repulsion in the closed-packed layer. Such a packing motif with equal adsorption sites but different intermolecular distances in the unit cell as well as different azimuthal alignments was identified previously for heptahelicene on Cu(111).[11]

Attractive intermolecular interactions clearly drive the first transition upon cooling and increase the binding enthalpy. Hence, the (4 0, 0 4) phase must have a higher entropy as a result of vibrational excitations.[17] Remarkably, the free corannulene molecule undergoes rapid bowl inversion at a rate of about 200 kHz at room temperature; bowl inversion ceases at 209 K.[18] The activation barrier for corannulene inversion was estimated to be 11.5 kcal mol^{-1} on the basis of NMR spectroscopic experiments with various derivatives.[19] The phase transitions occur in a temperature range in which the bowl-inversion rate approaches zero. An inversion in the adsorbed state would cause desorption (as observed for ammonia[20]). The degree of freedom of the inversion mode must be transformed into a frustrated vibration on the surface. DFT calculations identified the

inversion of the free molecule as the softest vibrational mode (see the Supporting Information). To mimic the vibrations in the adsorbed state, we carried out calculations for a single molecule with all carbon atoms of one hexagonal ring held fixed. This approach does not take any electronic influence of the surface into account. However, for corannulene on Cu(110), for example, no charge transfer was detected that would have a notable influence on vibration frequencies.[16] The calculated vibrational energies are compatible with the temperature range of the phase transitions (see Table T1 in the Supporting Information). These vibrations are breathing modes and require more space in the 2D lattice (Figure 4e). It is well accepted that the excitation of vibrations at higher temperatures leads to the occupation of more space; this effect was demonstrated recently for benzene.[21] The depopulation of vibrational states by means of cooling decreases the spatial requirements of the molecules and enables closer packing.[17]

We have shown that phase transitions can be tracked in great detail at the molecular level by scanning tunneling microscopy. This approach enabled us to identify periodic molecular movements in the supercooled crystal phase as the destabilizing dynamics at the onset of the phase transition and thus provided direct insight with molecular resolution into reversible phase transitions in 2D molecular crystals. The development of faster imaging techniques should lead to substantially more insight into the mechanism of crystallization phenomena at surfaces.

Experimental Section

Corannulene was evaporated at 373 K under ultrahigh vacuum from an effusion cell onto a copper single-crystal (MaTeK) surface at room temperature. The crystal surface was prepared by standard methods.[22] All STM images were recorded with an Omicron VT STM (Scala system) in constant-current mode at bias voltages (sample) from ± 250 to ± 3000 mV and tunneling currents from 25 to 2000 pA. A strong bias dependence of the contrast was only observed for small absolute bias values. STM parameters: Figure 1e (left to right): -710 mV, 50 pA, 558 nm s^{-1}, 253 K; $+1600$ mV, 250 pA, 651 nm s^{-1}, 230 K; -525 mV, 100 pA, 195 nm s^{-1}, 70 K; Figure 2: -1800 mV, 140 pA, 1627 nm s^{-1}, 69 K; Figure 4a: $+1800$ mV, 100 pA, 751 nm s^{-1}, 221 K; Figure 4c: $+1800$ mV, 100 pA, 601 nm s^{-1}, 221 K. All images were flattened only, except those in Figure 1, which were averaged by using a custom-made procedure. Conformational analysis of corannulene was carried out by using GAMESS.[23] See the Supporting Information for a detailed description of the methods used.

Received: September 16, 2008
Revised: November 22, 2008
Published online: February 11, 2009

Keywords: corannulene · phase transitions · polymorphism · scanning probe microscopy · self-assembled monolayers

[1] a) J. Bernstein, *Polymorphism in Molecular Crystals*, Oxford University Press, Oxford, **2002**; b) G. Desiraju, *Angew. Chem.* **2007**, *119*, 8492–8508; *Angew. Chem. Int. Ed.* **2007**, *46*, 8342–8356.

[2] a) J. Haleblian, W. McCrone, *J. Pharm. Sci.* **1969**, *58*, 911–929; b) S. Datta, D. J. W. Grant, *Nat. Rev. Drug Discovery* **2004**, *3*, 42–57.

[3] M. Wuttig, N. Yamada, *Nat. Mater.* **2007**, *6*, 824–832.

[4] a) F. Wöhler, J. von Liebig, *Ann. Pharm.* **1832**, *3*, 249–282; b) W. I. F. David, K. Shankland, C. R. Pulham, N. Blagden, R. J. Davey, M. Song, *Angew. Chem.* **2005**, *117*, 7194–7197; *Angew. Chem. Int. Ed.* **2005**, *44*, 7032–7035.

[5] N. N. Sirota, *Cryst. Res. Technol.* **1982**, *17*, 661–691.

[6] "Reversible" means that the crystal returns to the original phase. Particular molecules are not expected to return to their precise initial positions upon retransformation.

[7] F. H. Herbstein, *Acta Crystallogr. Sect. B* **2006**, *62*, 341–383.

[8] Y. V. Mnyukh, *Mol. Cryst. Liq. Cryst.* **1979**, *52*, 163–200.

[9] a) J. D. Dunitz, *Acta Crystallogr. Sect. B* **1995**, *51*, 619–631; b) J. D. Dunitz, *Pure Appl. Chem.* **1991**, *63*, 177–185.

[10] a) S. De Feyter, F. C. De Schryver, *Chem. Soc. Rev.* **2003**, *32*, 139–150; b) J. V. Barth, G. Costantini, K. Kern, *Nature* **2005**, *437*, 671–679; c) R. Fasel, M. Parschau, K.-H. Ernst, *Nature* **2006**, *439*, 449–452; d) S.-W. Hla, K.-H. Rieder, *Annu. Rev. Phys. Chem.* **2003**, *54*, 307–330; e) B. C. Stipe, M. A. Rezaei, W. Ho, *Science* **1998**, *280*, 1732–1735; f) H. C. Manoharan, C. P. Lutz, D. M. Eigler, *Nature* **2000**, *403*, 512–515.

[11] R. Fasel, M. Parschau, K.-H. Ernst, *Angew. Chem.* **2003**, *115*, 5336–5339; *Angew. Chem. Int. Ed.* **2003**, *42*, 5178–5181.

[12] Y.-T. Wu, J. S. Siegel, *Chem. Rev.* **2006**, *106*, 4843–4867.

[13] a) The transformation matrix (m_{11} m_{12}, m_{21} m_{22}) links the adsorbate lattice vectors (b_1, b_2) to the substrate lattice vectors (a_1, a_2): $\begin{pmatrix} b_1 \\ b_2 \end{pmatrix} = \begin{pmatrix} m_{11} & m_{12} \\ m_{21} & m_{22} \end{pmatrix} \begin{pmatrix} a_1 \\ a_2 \end{pmatrix}$ that is, $b_1 = m_{11}a_1 + m_{12}a_2$ and $b_2 = m_{21}a_1 + m_{22}a_2$; b) R. L. Park, H. H. Madden, *Surf. Sci.* **1968**, *11*, 188–202.

[14] a) T. Hashizume, K. Motai, X. D. Wang, H. Shinohara, Y. Saito, Y. Maruyama, K. Ohno, Y. Kawazoe, Y. Nishina, H. W. Pickering, Y. Kuk, T. Sakurai, *Phys. Rev. Lett.* **1993**, *71*, 2959–2962; b) J. A. Larsson, S. D. Elliot, J. C. Greer, J. Repp, G. Meyer, R. Allenspach, *Phys. Rev. B* **2008**, *77*, 115434.

[15] R. E. Reed-Hill, R. Abbaschian, *Physical Metallurgy Principles*, 3rd ed., PWS, Boston, **1991**.

[16] M. Parschau, R. Fasel, K.-H. Ernst, O. Gröning, L. Brandenberger, R. Schillinger, T. Greber, A. P. Seitsonen, Y.-T. Wu, J. S. Siegel, *Angew. Chem.* **2007**, *119*, 8406–8409; *Angew. Chem. Int. Ed.* **2007**, *46*, 8258–8261.

[17] A. I. Kitajgorodskij, *Acta. Crystallogr.* **1965**, *18*, 585–590.

[18] L. T. Scott, M. M. Hashemi, M. S. Bratcher, *J. Am. Chem. Soc.* **1992**, *114*, 1920–1921.

[19] T. J. Seiders, K. K. Baldridge, G. H. Grube, J. S. Siegel, *J. Am. Chem. Soc.* **2001**, *123*, 517–525.

[20] J. I. Pascual, N. Lorente, Z. Song, H. Conrad, H. P. Rust, *Nature* **2003**, *423*, 525–528.

[21] J. D. Dunitz, R. M. Ibberson, *Angew. Chem.* **2008**, *120*, 4276–4278; *Angew. Chem. Int. Ed.* **2008**, *47*, 4208–4210.

[22] K.-H. Ernst, D. Schlatterbeck, K. Christmann, *Phys. Chem. Chem. Phys.* **1999**, *1*, 4105–4112.

[23] M. W. Schmidt, K. K. Baldridge, J. A. Boatz, S. T. Elbert, M. S. Gordon, J. H. Jensen, S. Koseki, N. Matsunaga, K. A. Nguyen, S. Su, T. L. Windus, M. Dupuis, J. A. Montgomery, Jr., *J. Comput. Chem.* **1993**, *14*, 1347–1363.

